10.1007/s40684-015-0007-x

An Energy Conversion Model for Cantilevered Piezoelectric Vibration Energy Harvesters using Only Measurable Parameters

Jae Eun Kim[1], Hongjin Kim[2], Hansol Yoon[3], Yoon Young Kim[2], and Byeng D. Youn[2,#]

1 School of Mechanical and Automotive Engineering, Catholic University of Daegu, 13-13, Hayang-ro, Hayang-eup, Gyeongsan-si, Gyeongsangbuk-do, South Korea, 712-702
2 WCU Multiscale Design Division, School of Mechanical and Aerospace Engineering, Seoul National University, 1, Gwanak-ro, Gwanak-gu, Seoul, South Korea, 151-744
3 Institute of Technology, Doosan Infracore, 10, Suji-ro 112beon-gil, Suji-gu, Yongin-si, Gyeonggi-do, South Korea, 448-795
Corresponding Author / E-mail: bdyoun@snu.ac.kr, TEL: +82-2-880-1919, FAX: +82-2-883-0179

KEYWORDS: Energy harvesting, Piezoelectric, Energy conversion model, Vibration

Accurate predictions of the amount of harvestable energy available from ambient vibrations are important for design of energy harvesters and for their integration in specific applications. This need has motivated the development of many mathematical models for piezoelectric energy harvesters (PEHs). Existing models, however, require material and geometric PEH data that are often incorrect and/or unavailable. As a more accurate and practical means to meet this need, we propose an energy conversion model of a cantilevered PEH that requires only geometric data and modal parameters that can be directly measured using a standard vibration test. The newly proposed model facilitates calculation of the maximum output power and thus enables visualization of the harvestable energy from the target vibrating structure. Prediction accuracy of the proposed model was confirmed in our study through finite element analysis and experimental results. Practical use of the proposed energy conversion model was demonstrated by applying it to a cooling fan unit of a boiler facility in a power plant.

Manuscript received: August 9, 2014 / Revised: September 15, 2014 / Accepted: October 9, 2014

1. Introduction

Energy harvesting from ambient environments has been recognized as a promising powering technology that has the potential to replace batteries in wireless sensor networks (WSNs) and/or ubiquitous sensor networks (USNs).[1-3] Among various types of energy sources, mechanical vibration energy has received much attention due to its promising power density and ease of energy acquisition.[4-7] In this work, we are mainly concerned with piezoelectric energy harvesters (PEHs) because piezoelectricity is known to possess high energy conversion efficiency and ease of miniaturization.[7]

Although many improved configurations for PEHs have been proposed to overcome the main issues of insufficient output power and narrow working frequency bandwidth,[8-14] cantilever-type PEHs with relatively low resonant frequencies have been more commonly employed so far either in unimorph or bimorph configurations. It is noted that cantilever-type PEHs still play a role as a reference when the performance of a newly developed PEH are to be compared. Therefore, both 1) understanding of physical behaviors and 2) investigations of the effects of various parameters are important; thus, research to date has been mainly focused on the development of mathematical models for cantilevered PEHs. For example, the single-degree-of-freedom modeling approach (lumped parameter modeling) was developed by Roundy and Wright[15] duToit et al..[16] Since then, the variational principle combined with the Rayleigh-Ritz method[16,17] and the continuous distributed parameter approach[18,19] have been the two primary mathematical modeling approaches used to predict the electrical performance of cantilevered PEHs. More detailed discussions about the existing mathematical modeling approaches can be found in Erturk and Inman.[20] However, the modeling approaches mentioned so far have some limitations that inhibit their ability to correctly predict the output power of a PEH. These limitations occur because the mathematical models are based on the one-dimensional beam assumptions and thus cannot correctly assess the performance of plate-type PEHs that have large effective area for the energy harvesting. To address the issue, a plate finite element model[21] and an enhanced beam-based analysis model[22] were proposed, the latter of which also considered the distribution effects of a tip mass in contrast to the

conventional assumption of a concentrated tip mass. As an alternative to the above- mentioned modeling techniques, an equivalent electrical circuit method can be used to find DC electrical outputs as well as frequency-swept AC outputs.[23,24] Although significant advancements have been made in the field of PEH modeling, it is difficult to use the aforementioned models in cases where some of the electro-mechanical material properties required for analysis are unavailable or unreliable. Such is the case especially when ready-made commercial PEHs are to be used.

To overcome this difficulty, the work described in this paper aims at developing an energy conversion model that can easily predict the maximum amount of harvestable energy for a given PEH by using only basic measurable vibration parameters and geometric data. The prediction accuracy of the proposed model was confirmed in this work by examining it against the results from finite element analysis and the traditional PEH experiment. The PEH experiment is defined in this work as the standard procedure usually performed for a given PEH.[7] As a promising application of the proposed model, we examine its use to a harvestable energy map of a target vibrating structure, which is useful for.[25]

2. Derivation of a New Energy Conversion Model

We propose to derive an energy conversion model for cantilevered PEHs that is expressed in terms of measurable geometric and modal information such as resonant frequencies and damping ratios. The derivation starts with the well-developed electro- mechanically coupled governing equations for PEHs.

The electromechanically coupled governing equations - preferably at the fundamental vibration mode of a cantilevered PEH (see Fig. 1) based on the Rayleigh-Ritz method[17,22] - are expressed as:

$$M_{eq}\ddot{z}_{rel}(t)+C_{eq}\dot{z}_{rel}(t)+K_{eq}^{sc}z_{rel}(t)+\alpha\cdot V(t)=-M_rM_{eq}\ddot{z}_b \quad (1a)$$

$$\alpha\cdot z_{rel}(t)-C_p\cdot V(t)=-Q_e(t) \quad (1b)$$

where $Q_e(t)$ is generated charge on electrodes, $V(t)$ is the output voltage, C_p is the capacitance of the piezoelectric layer(s) at constant strain, α is the electromechanical coefficient, z_b denotes the base displacement, and z_{rel} is the displacement of a cantilever tip relative to a base. M_{eq}, C_{eq}, and K_{eq}^{sc} denote equivalent mass, damping, and stiffness, respectively. Note that M_r is a correction factor for a base-accelerated cantilever.[20,26] The symbols *sc* and *oc* are used to represent short-circuit and open-circuit conditions, respectively, throughout this work.

Note that piezoelectric vibration energy harvesters are preferably expected to operate at the short-circuit resonant frequency (f_{sc} in Hz).

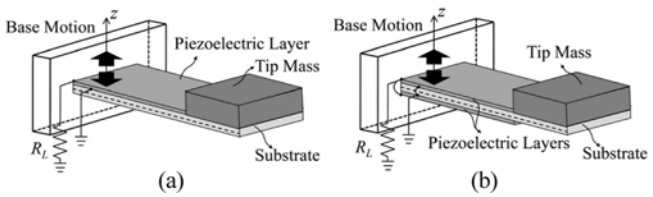

Fig. 1 Typical cantilevered PEHs in (a) unimorph and (b) bimorph (connected in parallel) configurations

This is because they experience a higher output current under almost the same output power seen at the open-circuit resonant frequency (f_{oc} in Hz). Therefore, the proposed energy conversion model is derived for the short-circuit resonance. The average output power across a load resistance R_L, which is calculated as $V^2/2R_L$, can be derived as (see, e.g.[22]):

$$P_{sc}^{out}(R_L)=\frac{1}{2}\cdot\frac{R_LM_r^2\alpha^2A_b^2}{(2\zeta_m\omega_{sc}^2C_pR_L)^2+(2\zeta_m\omega_{sc}+C_pR_Lk_{sys}^2\omega_{oc}^2)^2} \quad (2)$$

where A_b denotes the magnitude of the acceleration of a base excitation, ζ_m is the mechanical modal damping ratio measured at the short-circuit condition, and ω_{sc} (ω_{oc}) is the angular short-circuit (open-circuit) resonant frequency in rad/s. The parameter k_{sys}^2, which represents the electro-mechanical coupling coefficient (EMCC) of piezoelectric devices,[27] is defined as:

$$k_{sys}^2=\frac{\omega_{oc}^2-\omega_{sc}^2}{\omega_{oc}^2}=\frac{f_{oc}^2-f_{sc}^2}{f_{oc}^2} \quad (3)$$

Since the desired electrical output in the proposed energy conversion model is the maximum possible output power at the short-circuit resonance, the load resistance R_L is selected to be the internal impedance (R_L^{opt}) of a PEH at the short-circuit resonant frequency (see, e.g.[22]). This is given by:

$$R_L^{opt}=\frac{1}{\omega_{sc}C_p}\cdot\frac{2\zeta_m}{\sqrt{k_e^4+4\zeta_m^2}} \quad (4)$$

In the above equation, the new parameter k_e^2, called the expedient EMCC,[27] is introduced to simplify the subsequent derivation and the final form of the output power equation. The expedient EMCC is defined as:

$$k_e^2=\frac{k_{sys}^2}{1-k_{sys}^2}=\frac{f_{oc}^2-f_{sc}^2}{f_{sc}^2} \quad (5)$$

By substituting the above R_L^{opt} into Eq. (2), the maximum output power at the optimal load resistance under short-circuit resonance excitations is easily shown to be:[22]

$$P_{sc}^{\max}=\frac{M_r^2\alpha^2A_b^2}{8\zeta_m\omega_{sc}C_p(k_{sys}^2\omega_{oc}^2+\sqrt{4\omega_{sc}^4\zeta_m^2+k_{sys}^4\omega_{oc}^4})} \quad (6)$$

As mentioned earlier, the use of Eq. (6) for predicting the maximum output power requires correct information about the piezoelectric material properties of a PEH, such as the clamped dielectric permittivity ε^S for C_p and the piezoelectric stress constant e_{31} for α. The evaluation of the parameter α also depends on the degree of accuracy of an employed shape function that is integrated over the length of piezoelectric layer(s). In the case of a non- rectangular beam, it may be necessary to increase the number of employed shape functions[28] to enable accurate evaluation of α. Therefore, for accurate analysis of the maximum possible output power using the mathematical model in Eq. (6), the correct values of the mentioned parameters must be available. These values are then often subject to tuning by trial and error or through use of an optimization technique. In the worst case, where plate-type commercial PEHs with large width-to-length aspect ratios

are to be used, the well-developed beam-based mathematical models[17-19] become incorrect and the three dimensional finite element analyses should be employed. However, entire material properties required for piezoelectric finite element models are not usually provided by PZT vendors. Therefore, the maximum power output can be measured only by the PEH experiment, which includes the laborious load resistance sweep, as shown in Fig. 2.

Motivated by these observations, the work described here proposes an energy conversion model that requires no material properties. In order to circumvent the difficulty in obtaining the proper material properties often found in real-world settings, we propose to express Eq. (6) only in terms of easily measurable data, such as geometric and modal data acquired from a standard vibration test of a PEH. It is noted that Eq. (6) can also be applied to plate-type PEHs as long as the relevant parameters can be properly evaluated.[22] Therefore, starting from Eq. (6), it is transformed into the following equation after some manipulations:

$$P_{sc}^{\max} = \frac{1}{4}\frac{M_r^2 M_{eq} Q_m^2 k_e^2}{Q_m k_e^2 + \sqrt{1+Q_m^2 k_e^4}}\frac{A_b^2}{\omega_{sc}}$$

$$= \left[\frac{1}{2}\frac{M_r^2 M_{eq} Q_m^2 k_e^2}{Q_m k_e^2 + \sqrt{1+Q_m^2 k_e^4}}\right]_{PEH} \cdot \left[\frac{1}{2} V_b A_b\right]_{Excitaton} \quad (7)$$

where Q_m is the quality factor equal to $1/2\zeta_m$ and V_b denotes the amplitude of the velocity of a vibrating base. The above equation is arranged in two parts with each denoted by 'PEH' and by 'Excitation', respectively; one is related to the parameters of a PEH itself and the other to the external excitation environments. The term 'Excitation' then represents the mechanical input power per unit mass. In deriving the final form of Eq. (7), the following relation was employed:[22,24,29]

$$C_p = \frac{\alpha^2}{M_{eq}(\omega_{oc}^2 - \omega_{sc}^2)} = \frac{1}{k_e^2}\frac{\alpha^2}{\omega_{sc}^2 M_{eq}} = \frac{1}{k_e^2}\frac{\alpha^2}{K_{eq}} \quad (8)$$

In Eq. (7), the values of the equivalent mass (M_{eq}) and the correction factor (M_r) can be calculated as:[20,30]

$$M_{eq} = \frac{33}{104} M_b + M_t \quad (9)$$

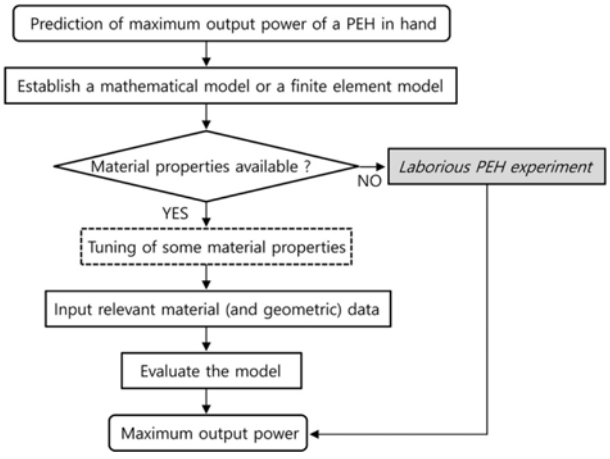

Fig. 2 Flow chart to emphasize the necessity of the proposed energy conversion model

$$M_r = \frac{(M_t/M_b)^2 + 0.603(M_t/M_b) + 0.08955}{(M_t/M_b)^2 + 0.4637(M_t/M_b) + 0.05718} \quad (10)$$

where M_b is the mass of a cantilevered PEH and M_t denotes the magnitude of a tip mass. The detailed procedure to derive Eq. (7) from Eq. (6) is explained in Appendix A.

Let us summarize the advantages of using Eq. (7) over Eq. (6):

- If any material properties are unavailable, Eq. (7) can still be effectively employed in the grey box in Fig. 2 because it requires only measurable (and derived) geometric (M_{eq} and M_r) and vibration parameters (ζ_m, f_{sc}, f_{oc} and A_b), i.e., no information on the values of C_p and α is required for Eq. (7), as mentioned earlier.
- The internal (denoted by 'PEH') and external (denoted by 'Excitation') contributions to the output power are explicitly expressed.
- Eq. (7) can be directly used to assess the amount of harvestable vibration energy in a specific vibration environment and thus it can be used to construct a harvestable energy map. Alternatively, the formula in Eq. (7) can be used to estimate the specifications of PEHs for a desired amount of harvested electrical energy once a vibration level denoted by 'Excitation' is known.

3. Output Power Prediction using the Proposed Energy Conversion Model

In order to validate the proposed energy conversion model, a standard vibration experiment was performed on a fabricated cantilevered PEH to obtain the parameters needed for Eq. (7).

For the cantilevered PEH in a unimorph type (as shown in Fig. 3), a piezoelectric layer (PSI-5H4E, Piezo Systems, Inc.) of 50×20×0.27 mm^3 is

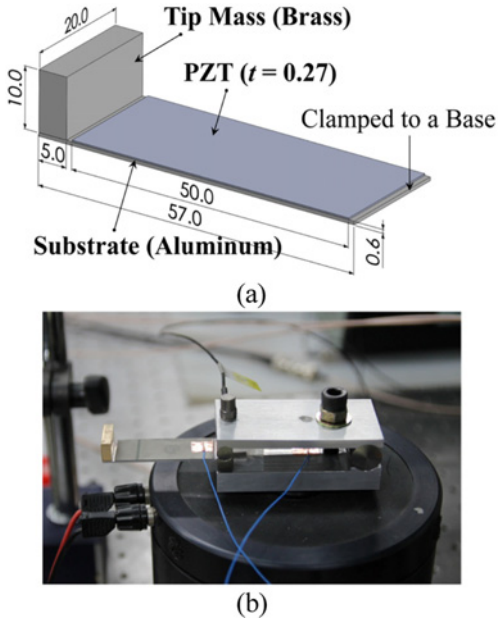

Fig. 3 (a) CAD model of a cantilevered PEH in the unimorph configuration with relevant dimensions in mm, and (b) the fabricated PEH installed on a vibration exciter in the zoomed-in experimental setup

bonded onto a 0.6 mm thick aluminum substrate using a conductive epoxy (CW2400, ITW Chemtronics). The tip mass is made of brass and weighs 8.4 g.

By employing the experimental procedure described in Erturk and Inman,[19] the short-circuit (f_{sc}) and open-circuit (f_{oc}) resonant frequencies in Hz were found to be 57.03 and 59.27, respectively. The modal damping ratio (ζ_m) was calculated by using the measured frequencies of half-power points, f_a and f_b. The acceleration, A_b, of the base structure measured by an accelerometer (4393, Brüel & Kjær) on the base structure was set to 1 m/s^2 at the short-circuit resonant frequency. The values of k_e^2, M_{eq}, and M_r were then calculated using Eqs. (5), (9) and (10), respectively. With all the required parameters tabulated in Table 1, we then calculated the maximum output power using Eq. (7):

$$P_{sc}^{\max}\big|_{\text{Eq.(7)}} = 112.14\ \mu\text{W}/(\text{m/s}^2)^2 \tag{11}$$

4. Verification using the PEH Experiment and Finite Element Analysis

4.1 Verification of Our Method using the PEH Experiment

In the standard procedure used to evaluate the performance of a PEH,[7] the open-circuit voltage and output voltage/power with a specified load resistance must be determined for varying excitation

frequencies. In addition, the output voltage/power at resonances for varying load resistances and output voltage/power at the optimal load resistance must be found for varying excitation frequencies.

In order to verify Eq. (7), the output power of a fabricated PEH was measured by changing external load resistances while the PEH was excited at the short-circuit resonance frequency. Fig. 4 shows a schematic of the experimental setup for the PEH experiment. The base structure was firmly mounted on an electromagnetic exciter (4809, Brüel & Kjær) and a function generator (33220A, Agilent Technologies) was used to generate an input sinusoidal signal at the short-circuit resonant frequency. The amplitude of the output voltage from the piezoelectric layer was measured using an oscilloscope

Table 1 Measured or calculated values of parameters for the fabricated PEH

Measured parameters				
f_{sc}	f_{oc}	f_a	f_b	A_b
57.03 Hz	59.27 Hz	56.1 Hz	57.9 Hz	1 m/s^2
Calculated parameters				
Q_m	k_{sys}^2	k_e^2	M_r	M_{eq}
31.6833	0.0742	0.0801	1.0584	0.0094 kg

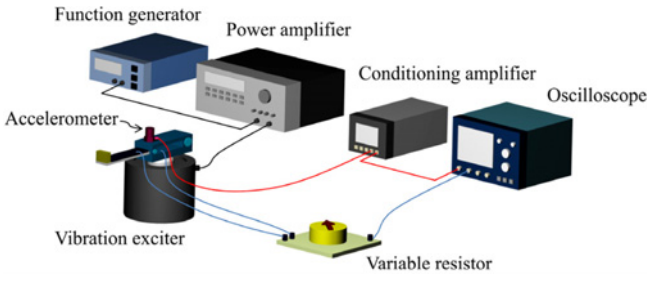

Fig. 4 Schematic of the experimental setup

(LT354M, LeCroy) for varying values of load resistance. From the results shown in Table 2, the maximum output power was found at the load resistance of 6 kΩ as:

$$P_{sc}^{\max}\big|_{\text{Experiment}} = 104.82\ \mu\text{W}/(\text{m/s}^2)^2 \tag{12}$$

The predicted value $P_{sc}^{\max}\big|_{\text{Eq.(7)}}$ from the proposed energy conversion model in Eq. (11) differs from $P_{sc}^{\max}\big|_{\text{Experiment}}$ in Eq. (12) by only 7.0% error.

4.2 Verification of Our Method using Finite Element Analysis

Next, the accuracy of our proposed energy conversion model was checked against the finite element analysis results obtained using ANSYS (Version 14.5). It is known that electrical outputs of a PEH with an attached load resistance can be well predicted using finite element analysis.[22] Here, the fabricated PEH was modeled with the three-dimensional coupled-field SOLID5 elements. The properties of the aluminum, brass and piezoelectric material used for the finite element analysis are listed in Table 3. For the piezoelectric material, the value of Poisson ratio is assumed to be 0.3, which is needed for estimating some material properties such as s_{12}^E, s_{13}^E, s_{44}^E, and s_{55}^E (see, e.g.[28]).

Table 2 Experimental results of the PEH performance tests for varying values of load resistance under excitations at the short-circuit resonant frequency

Resistance [kΩ]	Voltage [V/(m/s^2)]	Power [μW/(m/s^2)^2]
1	0.275	37.765
2	0.500	62.433
3	0.701	81.889
4	0.863	93.072
5	0.987	97.496
6	1.122	104.818 (max)
7	1.208	104.244
8	1.285	103.133
9	1.347	100.834
10	1.389	96.463
11	1.426	92.377

Table 3 Material properties of the tip mass, substrate, and piezoelectric material

	Aluminum (Substrate)		Brass (trip mass)
mass density (kg/m^3)	2700		8470
Young's modulus (Gpa)	69		110
Poisson's ratio	0.33		0.33
Piezoelectric material (PSI-5H4E, Piezo Systems, Inc.)			
mass density (kg/m^3)	7800	s_{11}^E (m^2/N)	1.61×10^{-11}
d_{15} (m/V)	7.41×10^{-10}	s_{12}^E (m^2/N)	-4.84×10^{-12}
d_{31} (m/V)	-3.20×10^{-10}	s_{13}^E (m^2/N)	-6.00×10^{-12}
d_{33} (m/V)	6.50×10^{-10}	s_{33}^E (m^2/N)	2.00×10^{-11}
ε_{11}^T (relative)	3800	s_{44}^E (m^2/N)	5.20×10^{-11}
ε_{33}^T (relative)	3800	s_{66}^E (m^2/N)	4.19×10^{-11}

Using mode-frequency analysis at the short-circuit and open-circuit conditions, f_{sc} and f_{oc} were found to be 57.91 Hz and 60.33 Hz, respectively. These values agree very well with the experimental results, 57.03 Hz and 59.27 Hz, as tabulated in Table 1. To find the maximum possible output power, the values of load resistance, R_L, were varied at the short-circuit resonant frequency. The output power was calculated by $V^2/2R_L$, where the magnitude of the output voltage (V) across an external load resistance (R_L) was determined using ANSYS simulations. The simulation results are shown in Fig. 5, together with the experimental results. The maximum output power was found at the short-circuit resonant frequency and the optimal impedance of 9.93 kΩ as:

$$P_{sc}^{\max}\big|_{\text{Finite element analysis}} = 109.31\ \mu\text{W}/(\text{m/s}^2)^2$$

In comparison with the above value of $P_{sc}^{\max}\big|_{\text{Finite element analysis}}$, the relative error in the maximum output power estimated by the proposed energy conversion model is only 2.6%. The deviation in Fig. 5 appears to result from manufacturing tolerance and measurement errors and also from the difficulty to realize the exact clamping condition.

5. Application of Our Proposed Model to a Harvestable Energy Map

As a promising application, an energy map[25] can be easily constructed using the proposed energy conversion model. Because this energy map helps to visualize harvestable ambient vibration energy distributions, it can be used to find the best places to locate PEHs. In doing so, the developed model will work as a practical and correct vibration-to-electric energy conversion model using the distributions of acceleration levels.

A cooling fan unit of a boiler facility at the power plant of Seoul National University was selected for the demonstration of green industry.[31] Fig. 6(a) shows the photograph of the cooling fan unit. The cooling fan housing, the drive belt cover, and the air duct were found to be dominantly excited at 38 Hz (due to the electric motor) and/or 452 Hz (due to the rotation of the cooling fan). The maximum acceleration was measured to be around 7 G (G = 9.81 m/s^2). In order to build a harvestable energy map for the cooling fan unit, a commercial bimorph PEH (T226-H4-503X, Piezo Systems, Inc) was considered. The PEH (T226-H4-503X) consists of two piezoelectric layers (top and bottom layers) and one substrate (center shim). The piezoelectric layers and substrate are PZT-5 H and brass, respectively. Each of the piezoelectric layers is 0.265 mm thick while the substrate is 0.140 mm thick. The overhang length and width of the PEH are 31.8 mm and 51 mm, respectively. The mass densities of the piezoelectric layer and substrate are 7,750 kg/m^3 and 9,000 kg/m^3, respectively, which are slightly different from those used in the previous verification model. The short-circuit and open-circuit resonant frequencies of T226-H4-503X were measured to be 122.4 Hz and 131.1 Hz, respectively. The value of Q_m was calculated to be 20.07. Under the given vibration condition, the excitation acceleration levels at selected locations were first measured. Using the distributions of acceleration levels, the maximum output power of T226-H4-503X was then estimated for the optimal external load resistance by Eq. (7). Note that all the locations for estimating the output power do not always have the highest peak values of acceleration at the short-circuit resonant frequency of a given PEH. Next, a harvestable vibration energy map, which was visualized on a CAD model, was constructed as shown in Fig. 6(b). Although the use of a harvestable energy map is not within the scope of this work, one can utilize the energy map to estimate the optimal locations for PEHs and the resulting harvestable energy from a finite number of installed PEHs.

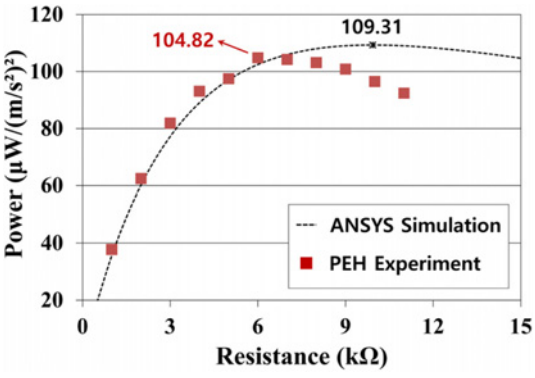

Fig. 5 Comparisons of the output power using finite element analysis and the PEH experiment for varying load resistance under the short-circuit resonance excitation

6. Conclusions

An alternative, practically useful energy conversion model for a cantilevered PEH was developed in this work. Unlike previous models, our model involves use of only the geometric and vibration parameters; both easily measured. The standard vibration modal test proved sufficient to evaluate the parameters in the proposed energy conversion model. The proposed model was shown to yield results within 7.0% of the

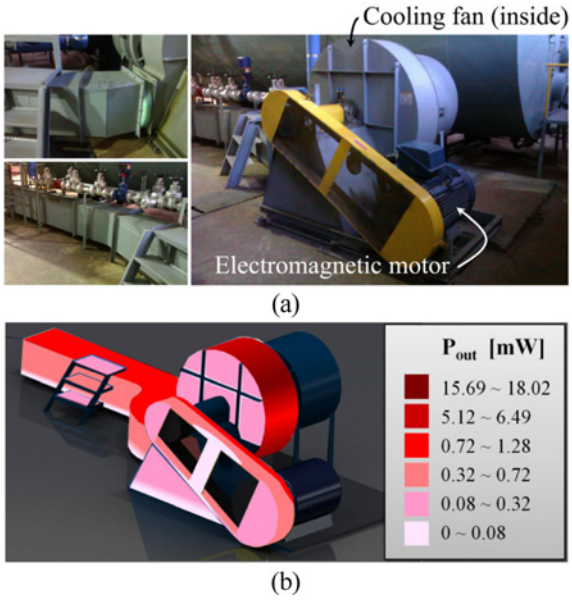

Fig. 6 (a) Cooling fan unit in a boiler facility as an example ambient vibration environment and (b) a visualized harvestable energy map on a CAD model of the unit where the proposed energy conversion model was used

results of the PEH experiment and within 2.6% errors of the results of a finite element simulation. Because the proposed model is more suitable for practical applications as compared with the more rigorous existing mathematical models, it could be favored for use in industrial sites. It is well acknowledged that randomness of the vibration[32] must be characterized for the practical use.

ACKNOWLEDGEMENT

This work was supported by POSCO Grant (No. 2011Z085) and also supported by Basic Science Research Program (No. 2011-0014430) and WCU Program (No. R31-2010-000-10083-0) through the National Research Foundation of Korea (NRF) funded by the Ministry of Education, Science and Technology.

REFERENCES

1. Roundy, S. and Wright, P. K., "A Piezoelectric Vibration Based Generator for Wireless Electronics," Smart Materials and Structures, Vol. 13, No. 5, pp. 1131-1142, 2004.
2. Hudak, N. S. and Amatucci, G. G., "Small-Scale Energy Harvesting through Thermoelectric, Vibration, and Radiofrequency Power Conversion," Applied Physics Letters, Vol. 103, No. 10, Paper No. 101301, 2008.
3. Priya, S. and Inman, D. J., "Energy Harvesting Technologies," Springer, 2009.
4. Roundy, S., Wright, P. K., and Rabaey, J., "A Study of Low Level Vibrations as a Power Source for Wireless Sensor Nodes," Computer Communications, Vol. 26, No. 11, pp. 1131-1144, 2003.
5. Sodano, H. A., Inman, D. J., and Park, G., "A Review of Power Harvesting from Vibration using Piezoelectric Materials," Shock and Vibration Digest, Vol. 36, No. 3, pp. 197-205, 2004.
6. Anton, S. R. and Sodano, H. A., "A Review of Power Harvesting Using Piezoelectric Materials (2003-2006)," Smart Materials and Structures, Vol. 16, No. 3, pp. R1-R21, 2007.
7. Erturk, A. and Inman, D. J., "Piezoelectric Energy Harvesting," John Wiley & Sons, 2011.
8. Kim, H. W., Batra, A., Priya, S., Uchino, K., Markley, D., et al., "Energy Harvesting using a Piezoelectric "Cymbal" Transducer in Dynamic Environment," Japanese Journal of Applied Physics, Vol. 43, No. 9A, pp. 6178-6183, 2004.
9. Kim, S., Clark, W. W., and Wang, Q.-M., "Piezoelectric Energy Harvesting with a Clamped Circular Plate: Analysis," Journal of Intelligent Material Systems and Structures, Vol. 16, No. 10, pp. 847-854, 2005.
10. Wang, S., Lam, K. H., Sun, C. L., Kwok, K. W., Chan, H. L. W., et al., "Energy Harvesting with Piezoelectric Drum Transducer," Applied Physics Letters, Vol. 90, No. 11, Paper No. 113506, 2007.
11. Wang, Z. and Xu, Y., "Vibration Energy Harvesting Device based on Air-Spaced Piezoelectric Cantilevers," Applied Physics Letters, Vol. 90, No. 26, Paper No. 263512, 2007.
12. Tang, L., Yang, Y., and Soh, C. K., "Toward Broadband Vibration-Based Energy Harvesting," Journal of Intelligent Material Systems and Structures, Vol. 21, No. 18, pp. 1867-1897, 2010.
13. Lee, S. and Youn, B. D., "A Design and Experimental Verification Methodology for an Energy Harvester Skin Structure," Smart Materials and Structures, Vol. 20, No. 5, Paper No. 057001, 2011.
14. Lee, S. and Youn, B. D., "A New Piezoelectric Energy Harvesting Design Concept: Multimodal Energy Harvesting Skin," Proc. of the IEEE Transactions on Ultrasonics, Ferroelectrics and Frequency Control, Vol. 58, No. 3, pp. 629-645, 2011.
15. Roundy, S., Wright, P. K., and Rabaey, J. M., "Energy Scavenging for Wireless Sensor Networks with Special Focus on Vibrations," Kluwer Academic Publishers, 2004.
16. duToit, N. E., Wardle, B. L., and Kim, S.-G., "Design Considerations for MEMS-Scale Piezoelectric Mechanical Vibration Energy Harvesters," Integrated Ferroelectrics, Vol. 71, No. 1, pp. 121-160, 2005.
17. Sodano, H. A., Park, G., and Inman, D., "Estimation of Electric Charge Output for Piezoelectric Energy Harvesting," Strain, Vol. 40, No. 2, pp. 49-58, 2004.
18. Erturk, A. and Inman, D. J., "A Distributed Parameter Electromechanical Model for Cantilevered Piezoelectric Energy Harvesters," Journal of Vibration and Acoustics, Vol. 130, No. 4, Paper No. 041002, 2008.
19. Erturk, A. and Inman, D. J., "An Experimentally Validated Bimorph Cantilever Model for Piezoelectric Energy Harvesting from Base Excitations," Smart Materials and Structures, Vol. 18, No. 2, Paper No. 025009, 2009.
20. Erturk, A. and Inman, D. J., "Issues in Mathematical Modeling of Piezoelectric Energy Harvesters," Smart Materials and Structures, Vol. 17, No. 6, Paper No. 065016, 2008.
21. De Marqui, Jr. C., Erturk, A., and Inman, D. J., "An Electromechanical Finite Element Model for Piezoelectric Energy Harvester Plates," Journal of Sound and Vibration, Vol. 327, No. 1, pp. 9-25, 2009.
22. Kim, J. E. and Kim, Y. Y., "Analysis of Piezoelectric Energy Harvesters of a Moderate Aspect Ratio with a Distributed Tip Mass," Journal of Vibration and Acoustics, Vol. 133, No. 4, Paper No. 041010, 2011.
23. Yang, Y. and Tang, L., "Equivalent Circuit Modeling of Piezoelectric Energy Harvesters," Journal of Intelligent Material Systems And Structures, Vol. 20, No. 18, pp. 2223-2235, 2009.
24. Kim, J. E., "Analysis of Vibration-Powered Piezoelectric Energy Harvesters by using Equivalent Circuit Models," Transactions of the Korean Society for Noise and Vibration Engineering, Vol. 20, No. 4, pp. 397-404, 2010.

25. Youn, B. D., Kim, J. E., Jo, C., Kim, Y. Y., Yoon, H., et al., "Harvestable Energy Scanner," KOR Patent, No. 10-2012-0139005, 2012.

26. Erturk, A. and Inman, D. J., "On Mechanical Modeling of Cantilevered Piezoelectric Vibration Energy Harvesters," Journal of Intelligent Material Systems and Structures," Vol. 19, No. 11, pp. 1311-1325, 2008.

27. Ikeda, T., "Fundamentals of Piezoelectricity," Oxford University Press, 1990.

28. Goldschmidtboeing, F. and Woias, P., "Characterization of Different Beam Shapes for Piezoelectric Energy Harvesting," Journal of Micromechanics and Microengineering, Vol. 18, No. 10, Paper No. 104013, 2008.

29. Richards, C. D., Anderson, M. J., Bahr, D. F., and Richards, R. F., "Efficiency of Energy Conversion for Devices Containing a Piezoelectric Component," Journal of Micromechanics and Microengineering, Vol. 14, No. 5, pp. 717-721, 2004.

30. Weaver, Jr. W., Timoshenko, S. P., and Young, D. H., "Vibration Problems in Engineering," John Wiley & Sons, 5th Ed., 1990.

31. Ahn, S.-H., "An Evaluation of Green Manufacturing Technologies Based on Research Databases," Int. J. Precis. Eng. Manuf.-Green Tech., Vol. 1, No. 1, pp. 5-9, 2014.

32. Yoon, H. and Youn, B. D., "Stochastic Quantification of the Electric Power Generated by a Piezoelectric Energy Harvester using a Time -Frequency Analysis under Non-Stationary Random Vibrations," Smart Materials and Structures, Vol. 23, No. 4, Paper No. 045035, 2014.

Appendix A

To help understand the proposed energy conversion model, a more detailed procedure to derive Eq. (7) from Eq. (6) is explained here.

Starting from Eq. (6), the use of Eq. (5) yields the following expression:

$$P_{sc}^{\max} = \frac{M_r^2 \alpha^2 A_b^2}{8\zeta_m \omega_{sc} C_p (k_e^2 \omega_{sc}^2 + \sqrt{4\omega_{sc}^4 \zeta_m^2 + k_e^4 \omega_{sc}^4})} = \frac{\alpha^2}{C_p} \cdot \frac{M_r^2 A_b^2}{8\zeta_m \omega_{sc}^3 (k_e^2 + \sqrt{4\zeta_m^2 + k_e^4})} \quad \text{(A.1)}$$

If the ratio of α^2/C_p from Eq. (8), which is equal to $k_e^2 \omega_{sc}^2 M_{eq}$, is substituted into the above equation, Eq. (A.1) is then expressed as

$$P_{sc}^{\max} = \frac{M_r^2 M_{eq} A_b^2 k_e^2}{8\zeta_m \omega_{sc} (k_e^2 + \sqrt{4\zeta_m^2 + k_e^4})} = \frac{M_r^2 M_{eq} k_e^2}{8\zeta_m (k_e^2 + \sqrt{4\zeta_m^2 + k_e^4})} \cdot \frac{A_b^2}{\omega_{sc}} \quad \text{(A.2)}$$

By replacing the mechanical damping ratio ζ_m with $1/2Q_m$, the first expression in Eq. (7) can now be rearranged as

$$P_{sc}^{\max} = \frac{1}{4} \cdot \frac{M_r^2 M_{eq} Q_m k_e^2}{k_e^2 + \sqrt{(1/Q_m)^2 + k_e^4}} \cdot \frac{A_b^2}{\omega_{sc}} = \frac{1}{4} \cdot \frac{M_r^2 M_{eq} Q_m^2 k_e^2}{Q_m k_e^2 + \sqrt{1 + Q_m^2 k_e^4}} \cdot \frac{A_b^2}{\omega_{sc}} \quad \text{(A.3)}$$